



HAL
open science

Effect of ions on sulfuric acid-water binary particle formation I: Theory for kinetic and nucleation-type particle formation and atmospheric implications

Joonas Merikanto, Jonathan Duplissy, Anni Määttänen, Henning Henschel, Neil M. Donahue, David Brus, Siegfried Schobesberger, Markku Kulmala, Hanna Vehkamäki

► To cite this version:

Joonas Merikanto, Jonathan Duplissy, Anni Määttänen, Henning Henschel, Neil M. Donahue, et al.. Effect of ions on sulfuric acid-water binary particle formation I: Theory for kinetic and nucleation-type particle formation and atmospheric implications. *Journal of Geophysical Research: Atmospheres*, 2016, 121 (4), pp.1736-1751. 10.1002/2015JD023538 . insu-01240821

HAL Id: insu-01240821

<https://insu.hal.science/insu-01240821>

Submitted on 21 Aug 2020

HAL is a multi-disciplinary open access archive for the deposit and dissemination of scientific research documents, whether they are published or not. The documents may come from teaching and research institutions in France or abroad, or from public or private research centers.

L'archive ouverte pluridisciplinaire **HAL**, est destinée au dépôt et à la diffusion de documents scientifiques de niveau recherche, publiés ou non, émanant des établissements d'enseignement et de recherche français ou étrangers, des laboratoires publics ou privés.

RESEARCH ARTICLE

10.1002/2015JD023538

This article is a companion to Duplissy *et al.* [2016] doi:10.1002/2015JD023539.

Key Points:

- Atmospheric binary particle formation can be both kinetic and nucleation-type
- Both ion-induced and neutral pathways are strong at free tropospheric conditions
- Ion-induced pathway dominates at midtroposphere and neutral at upper troposphere

Correspondence to:

J. Merikanto,
joonas.merikanto@fmi.fi

Citation:

Merikanto, J., J. Duplissy, A. Määttänen, H. Henschel, N. M. Donahue, D. Brus, S. Schobesberger, M. Kulmala, and H. Vehkamäki (2016), Effect of ions on sulfuric acid-water binary particle formation: 1. Theory for kinetic- and nucleation-type particle formation and atmospheric implications, *J. Geophys. Res. Atmos.*, 121, 1736–1751, doi:10.1002/2015JD023538.

Received 27 APR 2015

Accepted 31 AUG 2015

Accepted article online 8 SEP 2015

Published online 16 FEB 2016

Effect of ions on sulfuric acid-water binary particle formation: 1. Theory for kinetic- and nucleation-type particle formation and atmospheric implications

Joonas Merikanto^{1,2}, Jonathan Duplissy^{2,3}, Anni Määttänen⁴, Henning Henschel², Neil M. Donahue⁵, David Brus¹, Siegfried Schobesberger², Markku Kulmala², and Hanna Vehkamäki²

¹Finnish Meteorological Institute, Helsinki, Finland, ²Division of Atmospheric Science, Department of Physics, University of Helsinki, Helsinki, Finland, ³Helsinki Institute of Physics, University of Helsinki, Helsinki, Finland, ⁴Université Versailles St-Quentin, Sorbonne Universités, CNRS/INSU, LATMOS-IPSL, Guyancourt, France, ⁵Center for Atmospheric Particle Studies, Carnegie Mellon University, Pittsburgh, Pennsylvania, USA

Abstract We derive a version of Classical Nucleation Theory normalized by quantum chemical results on sulfuric acid-water hydration to describe neutral and ion-induced particle formation in the binary sulfuric acid-water system. The theory is extended to treat the kinetic regime where the nucleation free energy barrier vanishes at high sulfuric acid concentrations or low temperatures. In the kinetic regime particle formation rates become proportional to sulfuric acid concentration to second power in the neutral system or first power in the ion-induced system. We derive simple general expressions for the prefactors in kinetic-type and activation-type particle formation calculations applicable also to more complex systems stabilized by other species. The theory predicts that the binary water-sulfuric acid system can produce strong new particle formation in the free troposphere both through barrier crossing and through kinetic pathways. At cold stratospheric and upper free tropospheric temperatures neutral formation dominates the binary particle formation rates. At midtropospheric temperatures the ion-induced pathway becomes the dominant mechanism. However, even the ion-induced binary mechanism does not produce significant particle formation in warm boundary layer conditions, as it requires temperatures below 0°C to take place at atmospheric concentrations. The theory successfully reproduces the characteristics of measured charged and neutral binary particle formation in CERN CLOUD3 and CLOUD5 experiments, as discussed in a companion paper.

1. Introduction

Secondary particle formation through binary sulfuric acid-water nucleation has long been considered an important pathway for cloud condensation nuclei (CCN) production in the atmosphere, while nowadays formation mechanisms enhanced by other chemical species are known to contribute as well [Kerminen *et al.*, 2012]. Particle formation can also be enhanced by the presence of atmospheric ions. The uncertainties concerning the role of ions in particle formation have been one of the main motivations behind the Cosmics Leaving OUTdoor Droplets (CLOUD) experiments at CERN. The experiments show that ion-induced sulfuric acid-water particle formation cannot explain observed formation events at the ground level, even with further enhancement from ammonia [Kirkby *et al.*, 2011]. On the other hand, a potential boundary layer particle formation mechanism involving sulfuric acid and amines is not very sensitive to ion concentrations [Almeida *et al.*, 2013]. In the free troposphere, however, lower temperatures and higher atmospheric ionization rates offer much better conditions for significant binary particle formation. These regions also lack short-lived organic species that may significantly contribute to boundary layer particle formation.

Classical Nucleation Theory (CNT) is the standard theory that describes particle formation in supersaturated systems. It has been used for theoretical studies of binary sulfuric acid-water particle formation since the nominal work of Reiss [1950]. Refinements, like the inclusion of the effects of hydrate formation, have improved the predictive power of CNT compared to experiments, but the reliability of CNT in accurately describing particle formation in sulfuric acid-water system has remained questionable. Partly, this is due to the lack of experimental data but also due to intrinsic problems with the theoretical description. CNT has

been criticized for its reliance on the liquid drop model, which directly scales macroscopic bulk properties to molecular-sized clusters. It is well known that CNT cannot describe the thermodynamics of the smallest clusters accurately, and this deviation in the smallest scale can lead to very large errors in the particle formation rate calculations. Furthermore, the standard CNT for ion-induced binary system [Yue and Chan, 1979] has been criticized for the fact that it cannot differentiate between the enhancement of formation rates due to negative and positive ions [Lovejoy et al., 2004; Sorokin et al., 2006].

These shortcomings have promoted the development of more complex second-generation theoretical descriptions of charged particle formation in the sulfuric acid-water system, such as the schemes of Lovejoy et al. [2004] and Yu [2006, 2010], which are based on measured properties of neutral and charged clusters. However, the differences in the theoretical descriptions of these models lead to several orders of magnitude differences in predicted particle formation rates. For example, Lovejoy et al. [2004] predicted significant ion-induced binary particle formation in the midtroposphere but not within the boundary layer. Particle formation in the Yu [2006, 2010] model, on the other hand, is strong enough to explain observed particle formation also at ground level [Yu and Turco, 2011]. On the other hand, approaches based solely on quantum chemistry, such as the kinetic cluster size distribution model Atmospheric Cluster Dynamics Code [Olenius et al., 2013], cannot computationally deal with the very large difference between the concentrations of water and sulfuric acid at ambient conditions. Previous theoretical and experimental studies on sulfuric acid-water nucleation are briefly reviewed in the companion paper Duplissy et al. [2016] (hereafter referred to as Paper 2).

There is evidence from statistical mechanics that the failure of CNT results directly from its incorrect description of the smallest prenucleated clusters [Merikanto et al., 2007]. One of the oddities of CNT is, for example, that it predicts a finite formation work for a monomer cluster [Girshick and Chiu, 1990]. In the approach by Noppel et al. [2002], a single reference cluster with known properties from quantum chemistry calculations is used to correct the CNT-predicted formation rate. We will use a similar quantum chemistry-normalized form of CNT and extend the theoretical treatment into the kinetic regime where particle formation is no longer impeded by a free energy barrier. While our treatment considers only the binary system, it also serves as a conceptual basis for how sulfuric acid-based particle formation in a more general sense can be treated from a classical thermodynamic standpoint. In the companion paper (Paper 2) we carry out a full analysis of the CERN Cosmics Leaving Outdoor Droplets (CLOUD) experiments on neutral and ion-induced particle formation in the binary two-component sulfuric acid-water system, first discussed in Kirkby et al. [2011]. In this work (Paper 1) we describe the particle formation theory that is compared against experiments in Paper 2.

2. Theoretical Particle Formation in the Sulfuric Acid-Water and Sulfuric Acid-Water-Ion Systems

We use the quantum chemistry-normalized Classical Nucleation Theory, presented in Noppel et al. [2002] and Vehkamäki et al. [2002], to describe binary sulfuric acid-water particle formation. Here we extend the original theory to cover both neutral and ion-induced cases. The model applies quantum chemistry to solve the partitioning of sulfuric acid into free molecules (whose concentration defines the activity of sulfuric acid vapor) and sulfuric acid hydrates. In the present paper we use the most accurate results from electronic structure calculations [Kurten et al., 2007] in the determination of the sulfuric acid hydrate distribution. The cluster distribution in the nucleating vapor is normalized via a known reference concentration, which in Noppel et al. [2002] and Vehkamäki et al. [2002] was taken to be the sulfuric acid dihydrate concentration as discussed in more detail in section 2.3. The quantum chemically derived sulfuric acid monomer hydrate distribution is also here used as a reference to which CNT results are normalized in the case of neutral particle formation. However, here we use the full monomer hydrate distribution in the normalization process instead of only the dihydrate. This modified approach ensures a smooth transition into a one-component system in the pure sulfuric acid limit. In the ion-induced case the measured (Paper 2) air ion concentration acts as a natural reference concentration, as the collision frequency of sulfuric acid molecules with air ions is proportional to the air ion concentration. We extend the theoretical treatment into the kinetic regime where low temperatures or high sulfuric acid concentrations eliminate the free energy barrier. In the kinetic regime neutral particle formation is the formation of a sulfuric acid dimer and in the ion-induced case the formation of a sulfuric acid-ion pair. Throughout both papers we use the term “particle formation” to describe the generation of new particles from the vapor phase in general, and the term “nucleation,” which in the literature is often used synonymously, only when this process involves the crossing of a free energy barrier.

2.1. Sulfuric Acid Hydrate Distribution

Sulfuric acid and water molecules form strong hydrogen bonds due to the similar and bifunctional nature of the two types of molecules. Both can act as a hydrogen bond donor with two protons and acceptor for multiple hydrogen bonds. Already in a small cluster containing one sulfuric acid molecule and one water molecule, the water molecule can be involved in two hydrogen bonds. In a water-water dimer two hydrogen bonds are not possible due to geometric restrictions. An electric field introduced by an ion can increase the binding energy of sulfuric acid and water clusters helping to keep the molecules together. In a vapor containing sulfuric acid and water, the two species form hydrates that are bound molecular clusters containing at least one sulfuric acid molecule and some water molecules. Even though the free energy of binding between sulfuric acid and water is somewhat smaller than that between two molecules of sulfuric acid, the much higher (often 10 orders of magnitude) concentration of water compared to sulfuric acid under typical atmospheric conditions leads to clusters of one sulfuric acid with a few water molecules being much more common than clusters containing several molecules of sulfuric acid. The hydrates stabilize the vapor and lower theoretically calculated particle formation rates compared to a hypothetical case where all sulfuric acid molecules in the gas phase are assumed to be free monomers [Heist and Reiss, 1974; Jaecker-Voirol et al., 1987; Kulmala et al., 1991; Noppel et al., 2002]. For the particle formation rate calculations one must therefore first solve the distribution of sulfuric acid hydrates.

The total sulfuric acid concentration ρ_a^{total} is given by

$$\rho_a^{\text{total}} = \sum_{n_a=1}^{\infty} \sum_{n_w=0}^{\infty} \rho(n_a, n_w), \quad (1)$$

where $\rho(n_a, n_w)$ is the concentration of hydrates containing n_a sulfuric acid molecules and n_w water molecules. Due to the very large concentration difference under atmospheric conditions, the number of water molecules bound to hydrates is an insignificant fraction of the total number of water molecules and thus $\rho_w^{\text{total}} = \rho_w^{\text{free}} = \rho(0, 1)$ to a sufficient accuracy. The equilibrium hydrate distribution is given by

$$\rho(n_a, n_w) = (\rho_a^{\text{free}})^{n_a} (\rho_w^{\text{free}})^{n_w} (\rho_0)^{(1-n_a-n_w)} \exp\left(-\frac{\Delta H(n_a, n_w) - T\Delta S(n_a, n_w)}{RT}\right), \quad (2)$$

where T is the temperature, R is the molar gas constant, $\Delta H(n_a, n_w)$ and $\Delta S(n_a, n_w)$ are the molar enthalpy and entropy of formation of the (n_a, n_w) hydrate from isolated molecules, and ρ_0 is the reference concentration at which the formation enthalpy $\Delta H(n_a, n_w)$ and entropy $\Delta S(n_a, n_w)$ are reported. Equation (1) has to be solved iteratively when clusters containing more than one sulfuric acid molecule are accounted for, as the concentration of free sulfuric acid $\rho_a^{\text{free}} = \rho(1, 0)$ is not usually known from experiments but rather the total concentration of sulfuric acid ρ_a^{total} . We calculated the equation using enthalpies and entropies obtained from quantum chemical calculations for clusters containing up to four sulfuric acid molecules and five water molecules using the data from Henschel et al. [2014]. As expected, these calculations showed with high accuracy that only clusters with one sulfuric acid are significant when solving the partitioning of sulfuric acid into hydrates, and the hydrate distribution can be truncated after four water molecules (this result is also supported by results of Loukonen et al. [2010]). For this smaller set of hydrates, we use in our final calculations the reaction coefficients provided by Kurten et al. [2007], as they include an additional anharmonic correction term that makes a significant contribution to the calculation of reaction coefficients. In Paper 2 the measured sulfuric acid concentration ρ_a^{total} also corresponds to monomer (potentially hydrated) sulfuric acid (see section 2.2.4. in Paper 2).

2.2. Classical Nucleation Theory

In nucleation the phase transition proceeds through the crossing of a free energy barrier, whose size is obtained in the Classical Nucleation Theory (CNT) from the thermodynamic work of formation of the critical cluster. The critical cluster is the smallest cluster that is at least as likely to grow as to decay, and it is denoted by superscript asterisk. The theory employs the liquid drop model, where the nucleating cluster is considered as a small spherical embryo of a macroscopic phase that shares the same thermodynamic properties as the macroscopic liquid having the same composition. Due to the liquid drop model, the change in the work of formation is a smooth function of cluster radius, as the model neglects the molecular structure of the droplets.

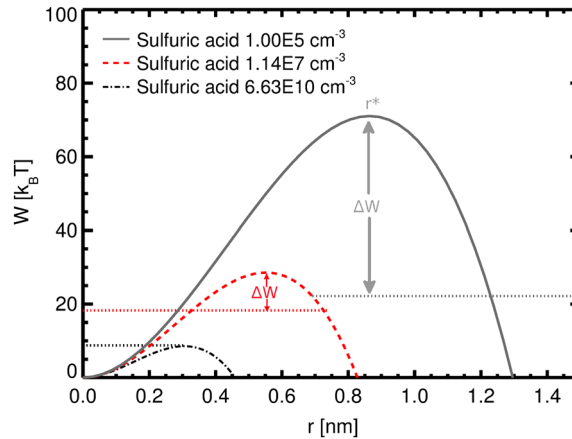


Figure 1. Work of formation as a function of cluster geometric radius with fixed composition $x_a = x_a^*$ for the neutral sulfuric acid-water nucleation at $T = 249.0$ K and $RH = 50\%$ for different ambient sulfuric acid concentrations (units of energy used here are $k_B T$, where k_B is the Boltzmann constant). The dotted lines show the work of formation of the reference cluster (sulfuric acid hydrate containing some fraction of water molecules) as given by CNT. The work of formation of the critical cluster, located at the top of the energy barrier, is calculated with respect to the reference cluster. At this temperature and relative humidity, the black dash-dotted line corresponds to condition (sulfuric acid concentration = $6.63 \times 10^{10} \text{ cm}^{-3}$) where particle formation becomes kinetically limited, i.e., the point where the critical cluster becomes identical with the reference cluster and contains exactly one sulfuric acid molecule and a fraction of water. The red dashed line corresponds to the conditions where neutral nucleation rate is $1 \text{ cm}^{-3} \text{ s}^{-1}$ (see Figure 7). The grey full line corresponds to the conditions where nucleation rate is negligible and is shown here to illustrate how the energy barrier grows with decreasing sulfuric acid concentration.

According to CNT, a general expression for the work of formation of a cluster having a radius r is given by [Yue and Chan, 1979; Laakso et al., 2002]

$$W(r, x_a) = -n_{a,\text{tot}} k_B T \ln \left(\frac{\rho_a^{\text{free}}}{\rho_{a,s}^{\text{free}}(x_a)} \right) - n_{w,\text{tot}} k_B T \ln \left(\frac{\rho_w^{\text{free}}}{\rho_{w,s}^{\text{free}}(x_a)} \right) + 4\pi r^2 \gamma(x_a) + \frac{q^2}{8\pi\epsilon_0} \left(1 - \frac{1}{\epsilon_r} \right) \left(\frac{1}{r} - \frac{1}{r_{\text{ion}}} \right), \quad (3)$$

where the total numbers of sulfuric acid and water molecules $n_{a,\text{tot}} = n_{a,c} + n_{a,s}$ and $n_{w,\text{tot}} = n_{w,c} + n_{w,s}$ include both bulk liquid ($n_{a,c}, n_{w,c}$) and surface excess ($n_{a,s}, n_{w,s}$) contributions, ϵ_0 and ϵ_r are the permittivities of the vacuum and the solution, respectively, r_{ion} is the radius of the ion if one exists, $\rho_{i,s}^{\text{free}}$ is the number concentration of free molecules of component i in a saturated vapor above a bulk solution with sulfuric acid mole fraction $x_a = \frac{n_{a,c}}{n_{a,c} + n_{w,c}}$, corresponding to the bulk core of the cluster, and γ is the composition-dependent surface tension.

The first two terms in equation (3) are proportional to the volume of the cluster, as the total numbers of molecules $n_{a,\text{tot}}$ and $n_{w,\text{tot}}$ are proportional to r^3 . These terms are negative and reduce the work of formation. The third term is positive and proportional to the surface area of the cluster, $4\pi r^2$. The fourth term is zero in case of neutral nucleation. In ion-induced nucleation, the last term is proportional to the electric potential of the ion that falls off as $1/r$ and is negative for $r > r_{\text{ion}}$. Because of this last term, the energy barrier falls off more rapidly with a growing radius for the clusters containing an ion than it does for neutral clusters.

$W(r, x_a)$ forms a curved free energy surface in composition and size space, and the critical cluster is located at the saddle point of this surface. It is easier to visualize the behavior of $W(r, x_a)$ as a function of cluster radius only, as shown in Figures 1 and 2 for clusters with fixed composition $x_a = x_a^*$. Then, the critical cluster is located at the top of the energy barrier, i.e., when

$$\left(\frac{\partial W(r^*)}{\partial r} \right)_{x_a=x_a^*, T} = 0. \quad (4)$$

From the above equation r^* turns out to be

$$r^* = \frac{2\gamma(x_a^*)v_f(x_a^*)}{k_B T \ln(\rho_i^{\text{free}}/\rho_{i,s}^{\text{free}})} \left[1 - \frac{q^2}{64\pi\epsilon_0\gamma(x_a^*)} \left(1 - \frac{1}{\epsilon_r} \right) \frac{1}{r^{*4}} \right], \quad (5)$$

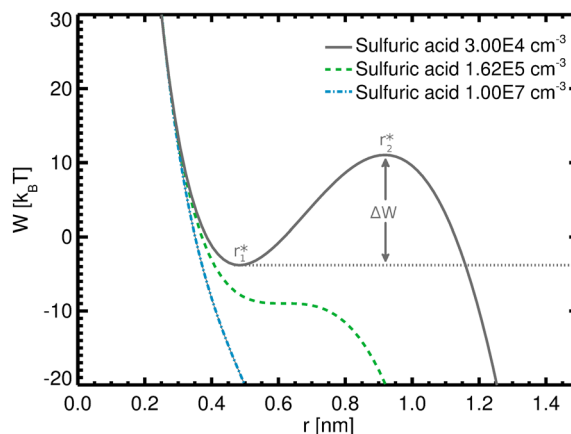


Figure 2. Work of formation as a function of cluster geometric radius with fixed composition $x_a = x_a^*$ for the ion-induced sulfuric acid-water particle formation at the same conditions ($T = 249.0$ K and $RH = 50\%$) as in Figure 1. The arrow between the full and dotted grey lines shows the work of formation of the critical cluster in ion-induced nucleation. The cluster at r_1^* contains the core ion with some sulfuric acid and water attached, and r_2^* cluster contains the ion at the core as well as additional sulfuric acid and water attached into it. Green dashed line stands for the sulfuric acid concentrations at which the ion-induced particle formation becomes kinetically limited at this temperature and relative humidity. Above this acid concentration ($1.62 \times 10^5 \text{ cm}^{-3}$) the work of formation does not have a local maximum anymore and the free energy surface along is reduced to a monotonically decreasing curve, as indicated by the blue dash-dotted line. The blue line corresponds to the conditions where ion-induced kinetic particle formation rate is $1 \text{ cm}^{-3} \text{ s}^{-1}$ if the ion concentration is equal to 300 ions cm^{-3} .

where i stands for either of the components (water or acid). The last term inside the square brackets is zero for neutral nucleation, and equation (5) has only one solution corresponding to the critical cluster. For ion-induced nucleation the equation has two or zero real solutions. If the number of solutions is two, the smaller value r_1^* represents the ion with some excess sulfuric acid and water molecules attached to it, located at the local minimum in the free energy surface, and the larger value r_2^* is the radius of the critical cluster, located at the local maximum of the free energy surface. Since the last term inside the square brackets in equation (5) is negative for the ion-induced nucleation, the critical cluster is larger for neutral nucleation than it is for ion-induced nucleation under same conditions. If the number of real solutions is zero, ion-induced particle formation takes place kinetically without any free energy barrier.

The composition of the critical cluster can be solved by setting the derivative of $W(r, x_a)$ with respect to x_a to zero. One can apply Gibbs adsorption isotherm to cancel the derivatives of the surface tension with the terms containing surface excess contributions. The resulting equation is

$$v_w(x_a^*) \ln \frac{\rho_a^{\text{free}}}{\rho_{a,s}^{\text{free}}(x_a^*)} = v_a(x_a^*) \ln \frac{\rho_w^{\text{free}}}{\rho_{w,s}^{\text{free}}(x_a^*)}, \quad (6)$$

from which the composition of the critical cluster, x_a^* , can be solved. This equation is valid for both electrically neutral and ion-induced nucleation [Thomson, 1906; Yue and Chan, 1979; Laakso et al., 2002].

In CNT both the neutral and ion-induced nucleation rates can be written as [Stauffer, 1976]

$$J = R_{av} Z \rho^* = |\lambda_1| \frac{1}{\sqrt{|\det W(r^*)|}} \rho^*, \quad (7)$$

where R_{av} is the average growth rate due to condensation rate of sulfuric acid and water, Z is the Zeldovich nonequilibrium factor related to the shape of the free energy barrier (influenced by the charge) in the vicinity of the critical cluster, and ρ^* is the number concentration of critical clusters in the vapor. An accurate derivation of the product $R_{av} Z$ is described in Määttä et al. [2007]. The product $R_{av} Z$, which can also be written as $|\lambda_1| \frac{1}{\sqrt{|\det W(r^*)|}}$, describes the nucleation flux through the critical cluster size in unit time. $|\lambda_1|$ is the negative eigenvalue of the product matrix $R^* D^*$. The matrix D^* contains the second derivatives of the formation free

energy $W(r^*)$ with respect to the number of molecules in the critical cluster (D_{aa}^* , D_{aw}^* , D_{ww}^*), which can be written as follows (for the rest of the paper we use $n_{a,tot} = n_a$ and $n_{w,tot} = n_w$):

$$D_{aa}^* \equiv \frac{d^2W(r^*)}{dn_a^2} = \frac{1}{2k_B T} \left[\frac{-v_a^2 \gamma}{2\pi r^{*4}} + \left(k_B T \frac{dA_a}{dx_a^*} \frac{1}{A_a} + 2 \frac{dv_a}{dx_a^*} \frac{\gamma}{r^*} + 2v_a \frac{d\gamma}{dx_a^*} \frac{1}{r^*} \right) \frac{n_{w,c}^*}{(n_{a,c}^* + n_{w,c}^*)^2} + \frac{q^2}{32\pi^2 \epsilon_0} \left(1 - \frac{1}{\epsilon_r} \right) \left(\frac{v_a^2}{\pi r^{*7}} - \frac{dv_a}{dx_a^*} \frac{n_{w,c}^*}{r^{*4} (n_{w,c}^* + n_{a,c}^*)^2} \right) \right], \quad (8)$$

$$D_{ww}^* \equiv \frac{d^2W(r^*)}{dn_w^2} = \frac{1}{2k_B T} \left[\frac{-v_w^2 \gamma}{2\pi r^{*4}} + \left(k_B T \frac{dA_w}{dx_w^*} \frac{1}{A_w} + 2 \frac{dv_w}{dx_w^*} \frac{\gamma}{r^*} + 2v_w \frac{d\gamma}{dx_w^*} \frac{1}{r^*} \right) \frac{n_{a,c}^*}{(n_{a,c}^* + n_{w,c}^*)^2} + \frac{q^2}{32\pi^2 \epsilon_0} \left(1 - \frac{1}{\epsilon_r} \right) \left(\frac{v_w^2}{\pi r^{*7}} - \frac{dv_w}{dx_w^*} \frac{n_{a,c}^*}{r^{*4} (n_{w,c}^* + n_{a,c}^*)^2} \right) \right], \quad (9)$$

and

$$D_{aw}^* = D_{wa}^* \equiv \frac{d^2W(r^*)}{dn_w dn_a} = \frac{1}{2k_B T} \left[\frac{-v_a v_w \gamma}{2\pi r^{*4}} + \left(k_B T \frac{dA_w}{dx_w^*} \frac{1}{A_w} + 2 \frac{dv_w}{dx_w^*} \frac{\gamma}{r^*} + 2v_w \frac{d\gamma}{dx_w^*} \frac{1}{r^*} \right) \frac{n_{w,c}^*}{(n_{a,c}^* + n_{w,c}^*)^2} + \frac{q^2}{32\pi^2 \epsilon_0} \left(1 - \frac{1}{\epsilon_r} \right) \left(\frac{v_a v_w}{\pi r^{*7}} - \frac{dv_w}{dx_w^*} \frac{n_{w,c}^*}{r^{*4} (n_{w,c}^* + n_{a,c}^*)^2} \right) \right], \quad (10)$$

where A_a and A_w are, respectively, the liquid phase activities of acid and water, $x_w^* = 1 - x_a^*$ is the mole fractions of water in the bulk cluster core, and v_w and v_a are the composition-dependent partial molar volumes of water and acid, respectively. The terms in equations (8)–(10) proportional to the square of charge of the ion, q^2 , are zero for neutral binary particle formation. Equations (8)–(10) do not contain the terms proportional to the surface excess molecules which would cancel the derivatives of the surface tension with the help of Gibbs adsorption isotherm as in the derivation of equation (6). Thus, the surface tension derivatives remain in expressions for D_{aa}^* , D_{ww}^* , and D_{aw}^* .

The matrix R^* contains the condensation coefficients describing the collisions of monomers and clusters of size (n_a, n_w) with the critical cluster:

$$R_{aa}^* = \sum_{n_a, n_w}^{N_c} n_a n_w (r^* + r)^2 \sqrt{8\pi k_B T \left(\frac{1}{m^*} + \frac{1}{m} \right)} \rho(n_a, n_w), \quad (11)$$

$$R_{ww}^* = \sum_{n_a, n_w}^{N_c} n_w n_w (r^* + r)^2 \sqrt{8\pi k_B T \left(\frac{1}{m^*} + \frac{1}{m} \right)} \rho(n_a, n_w), \text{ and} \quad (12)$$

$$R_{aw}^* = R_{wa}^* = \sum_{n_a, n_w}^{N_c} n_a n_w (r^* + r)^2 \sqrt{8\pi k_B T \left(\frac{1}{m^*} + \frac{1}{m} \right)} \rho(n_a, n_w). \quad (13)$$

The mass and the radius of the critical cluster are m^* and r^* , and m and r are the mass and the radius of the monomer or cluster colliding with the critical cluster. Above the cutoff size N_c (one acid and four water molecules in this study) the concentrations of the clusters are negligible and are not accounted for in the calculations.

2.3. QC-Normalized Classical Nucleation Theory

The largest caveat in CNT is that it solely relies on the macroscopic properties of nucleating species via the use of the liquid drop model. Standard CNT is also problematic since it does not satisfy the law of mass action [Wilemski and Wyslouzil, 1995]. Quantum chemistry (QC)-normalized Classical Nucleation Theory, first presented by Noppel *et al.* [2002], includes quantum chemistry predicted cluster concentrations in a manner that satisfies the law of mass action. It thus corrects the CNT predicted cluster distribution for the smallest sizes while maintaining the computational feasibility of the CNT model.

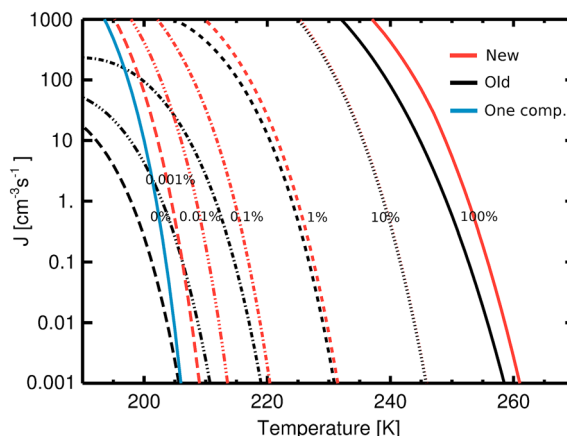


Figure 3. Theoretical neutral nucleation rates for sulfuric acid concentration 10^7 molecules cm^{-3} and relative humidities between $\text{RH} = 0\%$ and $\text{RH} = 100\%$ obtained using the dihydrate concentration as a reference cluster concentration $n, \rho_{\text{ref, neutral}} = \rho_{\text{hyd}}(1, 2)$ as in *Noppel et al. [2002]* and *Vehkamäki et al. [2002]* (black lines), or the new approach using $\rho_{\text{ref, neutral}} = \rho_{\text{hyd}}(1, n_w^*/n_a^*)$ (red lines). The blue line is obtained using self-consistent CNT for one-component sulfuric acid nucleation. The numbers over red or blue lines indicate the relative humidity in each case.

In CNT the nucleating vapor is assumed to be in a steady state, so that the number densities of different cluster species stay constant in time. Here we apply a concept of a reference concentration in order to discuss the neutral and ion-induced cases simultaneously. We write the steady state cluster concentration distribution as

$$\rho(n_a, n_w) = \rho_{\text{ref}} \exp \frac{-\Delta W^{\text{ref}}(n_a, n_w)}{k_B T}, \quad (14)$$

where ρ_{ref} is the concentration of reference clusters, and $\Delta W^{\text{ref}}(n_a, n_w)$ is the free energy difference, or the work of formation, between the reference cluster and the (n_a, n_w) cluster. In various applications of CNT different methods have been proposed for the selection of the reference concentration, while only some of them satisfy the law of mass action [*Wilemski and Wyslouzil, 1995*]. *Noppel et al. [2002]* took $\rho_{\text{ref, neutral}} = \rho_{\text{hyd}}(1, 2)$, so that the reference concentration in neutral sulfuric acid-water nucleation was the concentration of sulfuric acid dihydrates. This was done because the sulfuric acid dihydrate represented at the time the largest cluster with fairly well-known properties obtained from experiments, quantum chemistry, and data fitting. However, a selection of hydrate with fixed composition as a reference cluster leads to an inaccurate approach toward the pure sulfuric acid system as the relative humidity approaches zero. With the full quantum chemically derived monomer hydrate distribution up to a tetrahydrate in hand, we define the reference cluster concentration here as $\rho_{\text{ref, neutral}} = \rho_{\text{hyd}}(1, n_w^*/n_a^*)$, so that the reference cluster has the same relative amount of sulfuric acid and water as the critical cluster. As hydrates have integer numbers of water molecules attached to them, the reference cluster concentration is solved through linear interpolation between adjacent quantum chemically derived hydrate concentrations when n_w^*/n_a^* is not an integer number. Our cluster distribution returns the *Noppel et al. [2002]* distribution when the proportion of sulfuric acid to water in the critical cluster is the same as it is for a dihydrate (typically when RH is between 10% and 50%), and a self-consistent one-component sulfuric acid cluster distribution when there is no water in the critical cluster. Compared to the old *Noppel et al. [2002]* and *Vehkamäki et al. [2002]* model, the new approach returns close to identical nucleation rates at moderate RH , but higher rates when RH is either very low or close to 100%, as shown in Figure 3. The new approach also reduces to one-component sulfuric acid particle formation rates when RH tends to zero.

In QC-normalized CNT the work of formation of the critical cluster with respect to the reference cluster is obtained from equation (3) as

$$\Delta W_{\text{ref}}^* = W(r^*) - W(r_{\text{ref}}), \quad (15)$$

where $r_{\text{ref}} = r_1^*$ and $r^* = r_2^*$ for ion-induced nucleation. It should be noted that equations (5) and (15) do not depend on the size of the ion r_{ion} , and in equation (7) only the kinetic term R_{av} depends on the ion radius r_{ion} . This means that the size of the ion does not play a significant role in the formation rate calculation. In this work we set the radius of the ion to be $r_{\text{ion}} = 0.3$ nm. For neutral homogeneous binary nucleation r_{neutral}^* is the only solution of equation (5).

In the case of ion-induced nucleation we set $\rho_{\text{ref, ion-induced}} = \rho_{\text{ion}}$, so that the reference concentration is the concentration of ions obtained from experiments (in Paper 2) or a preselected value that describes the atmospheric ionization state (in Paper 1).

It should be pointed out that due to the applied liquid drop model in CNT, the numbers of molecules in the critical cluster are presented as real numbers instead of integers. Therefore, the change in the work of formation of the critical cluster is a smooth function of r instead of a discrete change. This can be viewed problematic when the critical cluster contains only a few molecules in highly supersaturated conditions. However, with the increasing supersaturation the change in the work of formation between adjacent clusters becomes smaller, and the free energy barrier becomes less steep. This may partly compensate for the error resulting from the continuum approach. Next, we look at what happens when supersaturation becomes so high that the free energy barrier disappears.

2.4. Particle Formation in the Kinetic Regime

If the gas phase concentration of the sulfuric acid is high enough, the nucleation free energy barrier vanishes entirely, after which particle formation is only limited by kinetics, i.e., by the condensation rate of vapor on the reference cluster. This type of collision-controlled particle formation has been described previously by McMurry and coworkers [McMurry, 1980, 1983; Rao and McMurry, 1989; Kuang et al., 2008; Zhang et al., 2010]. In our approach this takes place when ΔW_{ref}^* in equation (15) becomes zero. At this point it turns out that for the ion-induced nucleation $R_{\text{av}, Z_{\text{ion}}} \approx R_{a, \text{ion}}$, where $R_{a, \text{ion}}$ describes the condensation rate of sulfuric acid onto an air ion. Thus, at the kinetic limit, the ion-induced nucleation rate becomes with a good approximation equal to the collision rate of any sulfuric acid hydrate or free sulfuric acid molecule with the ion,

$$J_{\text{ion, kin}} \rightarrow \rho_{\text{ion}} \sum_{j=0}^{j_{\text{max}}} \left[\rho_{1,j} (r_{1,j} + r_{\text{ion}})^2 \sqrt{8\pi k_B T \left(\frac{1}{m_{1,j}} + \frac{1}{m_{\text{ion}}} \right)} \right]. \quad (16)$$

For the neutral particle formation ΔW_{ref}^* becomes zero and the kinetic limit is reached when the critical cluster equals our selected reference cluster. The critical cluster then contains only one sulfuric acid molecule and nominally some fraction of water molecules depending on the conditions. The particle formation rate at this point is to a good approximation described by the total collision rate between a sulfuric acid molecule or a hydrate with another sulfuric acid molecule or hydrate ($R_{\text{av}, Z_{\text{neutral}}} \approx R_{aa}$), so that

$$J_{\text{neutral, kin}} \rightarrow \sum_{j=0}^{j_{\text{max}}} \sum_{k=j}^{j_{\text{max}}} \left[\left(1 - \frac{\delta_{j,k}}{2} \right) \rho_{1,j} \rho_{1,k} (r_{1,j} + r_{1,k})^2 \sqrt{8\pi k_B T \left(\frac{1}{m_{1,j}} + \frac{1}{m_{1,k}} \right)} \right], \quad (17)$$

where $m_{1,j}$ is the mass of hydrate or sulfuric acid molecule, and $\delta_{j,k}$ is a delta function to avoid double counting the collisions between the same species. The equations above trace out the calculated formation rates at the kinetic limit under all conditions. This equation matches the dimer particle formation rate given by Zhang et al. [2010], which was calculated based on the collision-controlled nucleation theory of McMurry [1980].

The above equations (16) and (17) for the ion-induced and neutral kinetic particle formation are proportional to the first and second powers of sulfuric acid concentrations, respectively. Literature [e.g., Kulmala et al., 2006; Sipilä et al., 2010; Brus et al., 2011] refers to particle formation mechanisms proportional to the first power of the vapor (most often sulfuric acid) concentration as activation type and mechanisms proportional to the second power of the vapor concentration as kinetic type. Equations (16) and (17) can be simplified to shed light on the behavior of the prefactors in the collision-controlled activation-type and kinetic-type processes. No significant error in using equations (16) and (17) occurs if the summation over hydrate concentrations is replaced by the total sulfuric acid concentration. Then, activation-type particle formation is simply described as

$$J_{\text{ion, kin}} \equiv J_{\text{act}} = C \rho_{\text{pre}} \sqrt{T} [\text{H}_2\text{SO}_4] = A [\text{H}_2\text{SO}_4], \quad (18)$$

where in our case the number density of preexisting clusters $\rho_{\text{pre}} = \rho_{\text{ion}}$. Note that in a general collision-controlled “activation” case the preexisting cluster does not have to be charged. Similarly, the kinetic-type particle formation is described as

$$J_{\text{neutral, kin}} \equiv J_{\text{kin}} = \frac{C}{2} \sqrt{T} [\text{H}_2\text{SO}_4]^2 = K [\text{H}_2\text{SO}_4]^2, \quad (19)$$

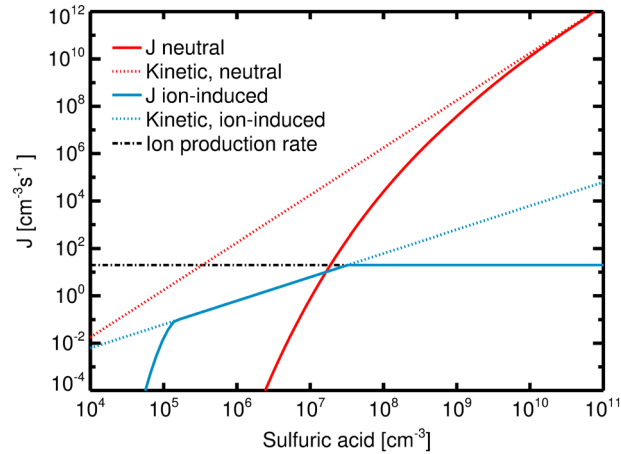


Figure 4. Neutral (red line) and ion-induced (blue line) particle formation rates as a function of sulfuric acid concentration at $T = 249.0$ K, $RH = 50\%$, $\rho_{\text{ion}} = 1000 \text{ cm}^{-3}$ and ion production rate of $20 \text{ cm}^{-3} \text{ s}^{-1}$. Dotted red and blue lines illustrate the kinetic limits for the neutral and ion-induced particle formation rates, respectively. Nucleation rates merge with the kinetic limits as they reach it at the point where the work of formation of the critical cluster becomes zero. Neutral nucleation rates can be very large before the kinetic limit due to the high concentration of sulfuric acid molecules. The black dash-dotted line represents the ion production rate, which poses an upper limit for the ion-induced particle formation rate.

with

$$C = (r_{1,0} + r_{\text{ref}})^2 \sqrt{8\pi k_B \left(\frac{1}{m_{1,0}} + \frac{1}{m_{\text{ref}}} \right)}, \quad (20)$$

where in our case $m_{\text{ref}} = m_{\text{ion}}$ (ion induced) or $m_{\text{ref}} = m_{1,0}$ (neutral), but these equations are general in nature; in the collision-controlled activation-type case the reference cluster concentration does not depend on the sulfuric acid concentration, whereas in the kinetic-type case the reference cluster concentration is proportional to the sulfuric acid concentration. The equations describe the physical basis of prefactors A and K that arise from the kinetic theory in conditions where no additional species are participating to the process and show that in the kinetic description the prefactors are proportional to square root of absolute temperature, \sqrt{T} , as also noted by *Zhang et al.* [2010] in case of neutral kinetic particle formation. In the rest of the paper we limit ourselves to discuss the barrierless and purely collision-limited particle formation simply as kinetic particle formation. The term activation is omitted from the rest of the manuscript, as in our description collision-controlled activation-type and kinetic-type mechanisms are simply similar barrierless particle formation processes.

The nucleation theorem [*Kashchiev, 1982*] relates the slope of the nucleation rate versus the concentration of a nucleating species in a log-log plot to the number of molecules of this species in the critical cluster. The theory is applicable to both homogeneous and ion-induced nucleation provided that the molecules of nucleating species are not dominantly bound to ions or other preexisting clusters [*Vehkamäki et al., 2012*]. As described by equation (7), $J = R_{\text{av}} Z \rho^*$ both for neutral ion-induced processes. Here Z is only a weak function of concentration and to a good approximation $R_{\text{av}} \propto \rho(1, 0)$. Therefore,

$$J \propto \rho(1, 0) \rho_{\text{ref}} \exp \left[-\frac{W^* - W_{\text{ref}}}{k_B T} \right], \quad (21)$$

where $\rho_{\text{ref}} \propto \rho(1, 0)$ in the neutral case, whereas in ion-induced case the ion production rate, and hence the number of ions, does not depend on the sulfuric acid concentration. Then,

$$\left(\frac{\partial \ln J_{\text{neutral}}}{\partial \ln \rho_a^{\text{free}}} \right) \approx 2 + (n_a^* - n_a^{\text{ref}}) \quad (22)$$

and

$$\left(\frac{\partial \ln J_{\text{ion}}}{\partial \ln \rho_a^{\text{free}}} \right) \approx 1 + (n_a^* - n_a^{\text{ref}}), \quad (23)$$

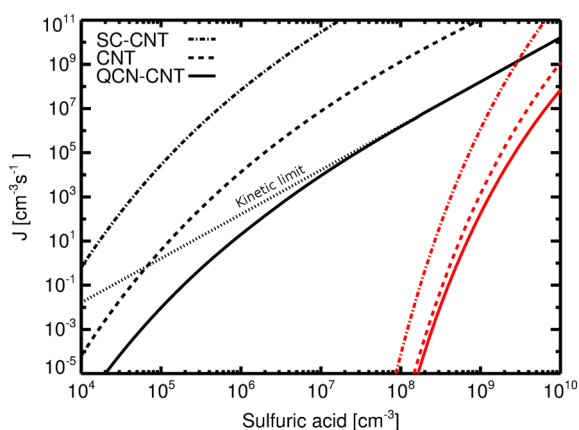


Figure 5. Comparison of the neutral binary formation rates predicted by standard hydrate-corrected CNT [Reiss, 1950; Jaeger-Voirol et al., 1987] (dash-dotted line), self-consistent CNT [Wilemski and Wyslouzil, 1995] (dashed line), and QC-normalized CNT (full line) for the neutral binary system with RH = 50% at 220 K (black) and 280 K (red).

where $(n_a^* - n_a^{\text{ref}})$ is the excess number of sulfuric acid molecules between the critical cluster and the reference cluster that should vanish at the kinetic limit. This is not exactly true for ion-induced nucleation, where at the kinetic limit the minima and the maxima in the free energy surface vanish into a plateau instead of a point in this surface. However, $(n_a^* - n_a^{\text{ref}})$ approaches zero rapidly as the kinetic limit is approached and differs from zero by a number less than unity at the kinetic limit. Therefore, the nucleation theorem further justifies the proportionality of equations (16) and (17) to sulfuric acid concentration and their use in the kinetic regime. Figure 4 shows the behavior of formation rates in different cases as a function of sulfuric acid concentration on a logarithmic scale. $J_{\text{ion,kin}}$ has a slope of one, and $J_{\text{neutral,kin}}$ has a slope of two. It should be noted that as reported in Ehrhart and Curtius [2013] and Kupiainen-Määttä et al. [2014], the nucleation theorem is often not practically applicable to identification of the critical cluster size from experimental data as, for example, losses of clusters to walls or preexisting particle surfaces, or ion-ion recombination, distort the analysis severely even in the simple binary water-sulfuric acid system.

2.5. Comparison With Standard and Self-Consistent CNT

Figure 5 shows the comparison of formation rates between the standard hydration-corrected CNT for the neutral binary system [Reiss, 1950; Jaeger-Voirol et al., 1987], the self-consistent neutral binary CNT [Wilemski and Wyslouzil, 1995], and QC-normalized CNT as presented here. The hydrate correction and the kinetic prefactor $R_{\text{av}}Z$ are calculated identically in each case. By using our notation, the standard CNT of Reiss [1950] is obtained by setting $\rho_{\text{ref,neutral}} = \rho_a^{\text{total}} + \rho_w^{\text{total}}$ and $W_{\text{ref}} = 0$ in equations (14) and (15) calculated for the critical cluster. The self-consistent binary CNT of Wilemski and Wyslouzil [1995] is obtained by setting $\rho_{\text{ref,neutral}} = x_a \rho_{a,s}^{\text{total}} + x_w \rho_{w,s}^{\text{total}}$, and $W_{\text{ref}} = x_a A_{1,a} \gamma_a + x_w A_{1,w} \gamma_w$, where $A_{1,j}$ and γ_j are the pure component monomer surface areas and surface tensions, respectively. The figure shows that both the standard and self-consistent rates can exceed the kinetic limit for the neutral system (sulfuric acid dimer formation rate) at high acid concentrations or low temperatures. The temperature dependence of neutral binary particle formation rates in QC-corrected CNT is lower than that for the standard or self-consistent binary CNT. Standard CNT is known to often produce too strong a temperature dependence of particle formation rates compared to experiments.

2.6. Thermodynamic Data

The thermodynamical parameters of the substances, such as the surface tension, the density of the solution, and the equilibrium vapor pressures over a flat (solution) surface, need to be known to solve the critical cluster properties and to calculate the nucleation rate. Most of the thermodynamical parameterizations we use are given in Vehkamäki et al. [2002] and summarized in Table 1. As noted in Vehkamäki et al. [2002], we need to extrapolate these parameters to low temperatures (< 230 K) outside the experimental data range. However, the low-temperature behavior of the extrapolated parameters is smooth with no obviously unphysical kinks.

The only thermodynamic property for which we used a different value than Vehkamäki et al. [2002] was the equilibrium vapor pressure of water vapor over (possibly supercooled) liquid water. We use the Wexler [1976] formulation for temperatures above 273.15 K and the equation from Murphy and Koop [2005] for temperatures

Table 1. Thermodynamical Data for the Sulfuric Acid-Water System^a

Parameter	Experiments	Fit	T Range
$P_{w,e}(T)$		<i>Wexler</i> [1976]	273–373 K
		<i>Murphy and Koop</i> [2005]	< 273 K
$P_{a,e}(T)$	<i>Ayers et al.</i> [1980]		338–445 K
		<i>Kulmala and Laaksonen</i> [1990]	153.15–363.15 K
		<i>Noppel et al.</i> [2002]	
$\sigma(x_a, T)$	<i>Sabinina and Terpugow</i> [1935] <i>Morgan and Davies</i> [1916] <i>Suggitt et al.</i> [1949] <i>Hoffmann and Seeman</i> [1960] <i>Myhre et al.</i> [1998]	<i>Vehkamäki et al.</i> [2002]	233–323 K
$\rho(x_a, T)$	<i>National Research Council</i> [1928] <i>Myhre et al.</i> [1998]	<i>Vehkamäki et al.</i> [2002]	273–373 K 220–300 K
$\mathcal{A}_g(x, T), \mathcal{A}_w(x, T)$		<i>Zeleznik</i> [1991]	220–350 K

^aThe data have been extrapolated below their temperature ranges, as mentioned also in *Vehkamäki et al.* [2002].

below 273.15 K as we needed to make sure that the equations behave well in subfreezing temperatures, and the *Murphy and Koop* [2005] equation is currently the best reference for the equilibrium vapor pressure over supercooled water.

3. Behavior of Modeled Particle Formation Rates as a Function of Atmospheric Parameters

According to the theory, particle formation in the sulfuric acid-water and sulfuric acid-water-ion systems can take place in two ways:

1. In conditions mildly supersaturated with sulfuric acid, particle formation can take place through nucleation, with a free energy barrier between the old (vapor) and the new (liquid) phase.
2. In highly supersaturated conditions, particle formation takes place in the kinetic regime, where every molecular collision between two sulfuric acid molecules or between sulfuric acid and an atmospheric ion leads to a freely growing embryo of a new phase. Neutral particle formation in the kinetic regime is collision-controlled formation of sulfuric acid dimers (the rate being proportional to the second power of the sulfuric acid concentration), whereas the ion-induced process in the kinetic regime is collision-controlled formation of sulfuric acid-ion pairs (the rate being proportional to the first power of sulfuric acid concentration).

The theory predicts that both nucleation and kinetic regimes are important under the experimental conditions at CLOUD3 and CLOUD5 as well as in the real atmosphere. Ion-induced particle formation is always energetically preferred to neutral particle formation due to its lower free energy barrier in the nucleation regime and due to its ability to reach the kinetic regime at lower sulfuric acid concentrations. However, atmospheric ion concentrations and production rates are always far lower than those for sulfuric acid. The typical atmospheric ion pair production rates due to cosmic rays vary between $2 \text{ cm}^{-3} \text{ s}^{-1}$ at the ocean surface and about $30 \text{ cm}^{-3} \text{ s}^{-1}$ at 11 km height, and these rates vary according to geomagnetic latitude and solar activity [*Bazilevskaya et al.*, 2008; *Usoskin et al.*, 2010], producing ion concentrations spanning from some hundreds cm^{-3} at ocean surface to some thousands cm^{-3} in the free troposphere. For comparison, atmospheric gas phase sulfuric acid production is mainly driven by photochemical reactions with typical production rates between 10^3 and $10^5 \text{ molecules cm}^{-3} \text{ s}^{-1}$ and concentrations between 10^5 and $10^7 \text{ molecules cm}^{-3}$ throughout the troposphere [*Eisele and Tanner*, 1993; *Pierce and Adams*, 2009; *Mikkonen et al.*, 2011; *Pierce et al.*, 2013]. These production rates set upper limits for the steady state particle formation rates. In atmospheric conditions it is possible that the production rates themselves become the limiting factors for the particle formation rates, particularly in case of ion-induced particle formation.

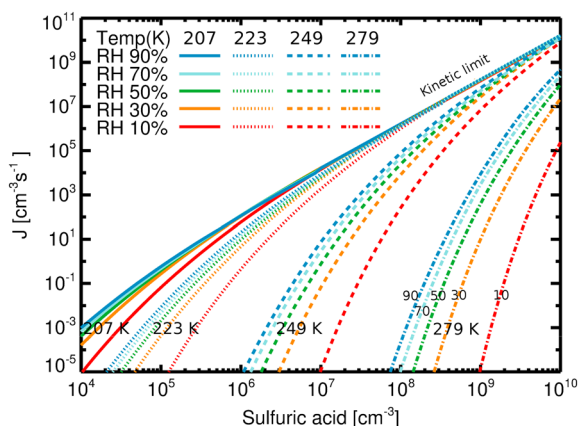


Figure 6. The effect of temperature and relative humidity on theoretical neutral binary particle formation rates against sulfuric acid concentration at temperatures corresponding to conditions in the CLOUD3 and CLOUD5 experiments (Paper 2). In the nucleation regime both temperature and relative humidity can strongly affect the formation rates. With a growing sulfuric acid concentration the effects of relative humidity and temperature on the formation rates become smaller as the particle formation approaches the kinetic regime. Note that often the particle formation rates at different temperatures are shown against supersaturation or activity, and these rates typically increase with temperature. The apparent, opposite trends shown here do not contradict the common understanding but are a consequence of plotting the rates against concentration instead of activity.

For the ion pair production rate the following balance equation must hold in a steady state:

$$q_{\text{ion}} = \text{Coag}S\rho_{\text{ion}} + \alpha\rho_{\text{ion}}^2 + J_{\text{ion}}, \quad (24)$$

where q_{ion} is the ion production rate (i.p.r.), and the right-hand side of the equation contains the loss terms where $\text{Coag}S\rho_{\text{ion}}$ represents the scavenging of ions due to coagulation onto preexisting particles, $\alpha\rho_{\text{ion}}^2$ accounts for ion-ion recombination, and J_{ion} is the ion-induced particle formation rate. Due to this limitation the dominant particle formation pathway can switch from ion-induced particle formation to neutral particle formation as the sulfuric acid concentration rises.

The effects of relative humidity, temperature, and sulfuric acid concentration on the neutral and ion-induced theoretical particle formation rates are illustrated in Figures 6 and 7. In both cases, as the free energy barrier vanishes at high sulfuric acid concentrations and particle formation takes place in the kinetic regime, formation rates become weakly dependent on temperature (\sqrt{T} dependence), and very weakly dependent on relative humidity (minor hydrate effects on collisional cross sections). At lower sulfuric acid concentrations particle formation is impeded by the free energy barrier, and formation rates are sensitive to temperature and relative humidity. Figure 7 also indicates the upper limit of the steady state particle formation set by the ion production rate. Both for neutral and ion-induced cases the nucleation rate can increase from effectively zero to more than $1 \text{ cm}^{-3} \text{ s}^{-1}$ when changing the relative humidity from 10% to 90%. However, in the kinetic regime the dependence of particle formation rate on relative humidity vanishes.

Figure 8 illustrates how neutral and ion-induced sulfuric acid-water particle formation takes place according to the theory in atmospheric conditions (assuming fixed RH = 50%, ion concentration of 4000 cm^{-3}). Figure 8 is divided into colored areas on top and white areas at the bottom by the line of significance that represents the minimum sulfuric acid concentration required for producing atmospherically relevant particle formation rates of $1 \text{ cm}^{-3} \text{ s}^{-1}$. This threshold for relevant particle formation is arbitrary, as smaller rates may be relevant depending on the conditions. However, it is a useful guideline since particle formation likely takes place in short-period bursts, or events, in the free troposphere, and in the boundary layer, reflecting the temporal variation in the ambient sulfuric acid concentration. In the white areas particle formation rates are lower than $1 \text{ cm}^{-3} \text{ s}^{-1}$.

The full red area in Figure 8 describes conditions for which neutral particle formation is both kinetic and taking place at rates above $1 \text{ cm}^{-3} \text{ s}^{-1}$. In the kinetic regime neutral particle formation rates are proportional to second power of the sulfuric acid concentration and to the square root of absolute temperature. Sulfuric acid concentration needs to be roughly 10^5 cm^{-3} for the collision rate between two sulfuric acid

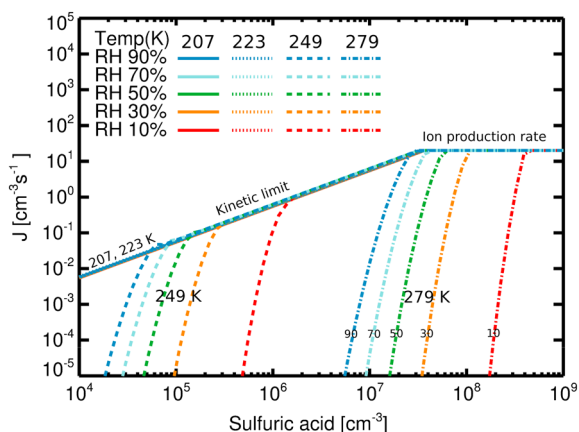


Figure 7. The effect of temperature and relative humidity on theoretical ion-induced particle formation rates against sulfuric acid concentration at temperatures corresponding to conditions in the CLOUD3 and CLOUD5 experiments. The ion concentration and ion production rate are taken to be 1000 cm^{-3} and $20 \text{ cm}^{-3} \text{ s}^{-1}$, respectively. For the two lowest temperatures particle formation is kinetic under these conditions, and the formation rates are equal to the collision frequency between ions and sulfuric acid molecules. The rates at higher temperatures also tend toward the collision frequency as the nucleation free energy barrier diminishes. All formation rates are ultimately limited by the ion production rate (minus the sink terms that are neglected in this figure).

molecules or hydrates to be $1 \text{ cm}^{-3} \text{ s}^{-1}$. The slight downward slope in the sulfuric acid concentration required for $J = 1 \text{ cm}^{-3} \text{ s}^{-1}$ around $T = 180 \text{ K}$ region is due to square root of T dependence of particle formation rates in the kinetic regime. At sulfuric acid concentrations below 10^5 cm^{-3} neutral particle formation can take place kinetically but with smaller formation rates than $1 \text{ cm}^{-3} \text{ s}^{-1}$, described by the white area at the left corner of Figure 8. The black dash-dotted line describes the sulfuric acid concentration above which neutral

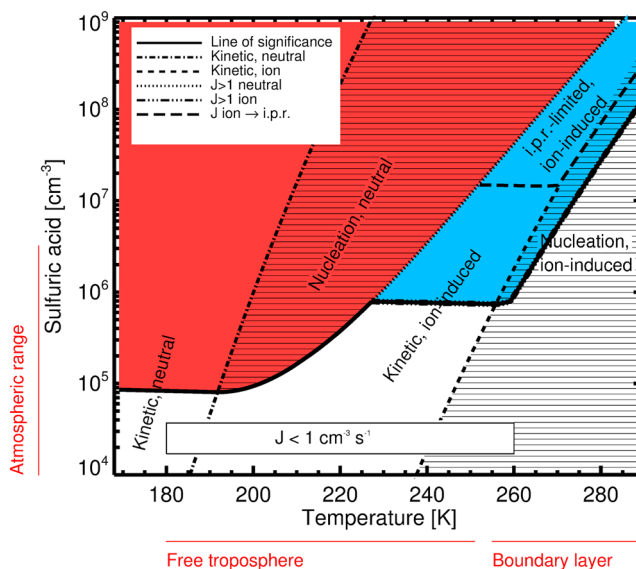


Figure 8. Theoretical neutral and ion-induced binary particle formation at various atmospheric conditions for a fixed relative humidity $\text{RH} = 50\%$, ion production rate of $20 \text{ cm}^{-3} \text{ s}^{-1}$, and ion concentration of 4000 cm^{-3} . The figure shows the conditions where neutral binary (red area) or ion-induced binary (blue area) particle formation mechanisms are dominant. In hatched regions particle formation takes place through the crossing of a free energy barrier (nucleation), and in full-colored regions particle formation is barrierless (kinetic). The line of significance (full line) separating the red and blue regions from the white regions shows the minimum sulfuric acid concentration above which the formation rate is larger than $1 \text{ cm}^{-3} \text{ s}^{-1}$. Long-dashed line shows the region above which ion-induced particle formation is limited by the ion production rate (i.p.r.) of $20 \text{ cm}^{-3} \text{ s}^{-1}$. Because ion-induced particle formation is directly proportional to the number of ions, dash-dot-dot-dot line represents $J = 1 \text{ cm}^{-3} \text{ s}^{-1}$ for $4000 \text{ ions cm}^{-3}$ as well as the formation rate of $0.1 \text{ cm}^{-3} \text{ s}^{-1}$ for 400 ions cm^{-3} .

particle formation takes place kinetically. This can happen at the conditions met in the upper troposphere and in the stratosphere.

The hatched red area corresponds to a region where neutral particle formation takes place through nucleation and at rates higher than $1 \text{ cm}^{-3} \text{ s}^{-1}$. The neutral formation rates in this region are a steep function of sulfuric acid concentration. The red regions show the temperatures and sulfuric acid concentrations above which neutral particle formation rate exceeds $1 \text{ cm}^{-3} \text{ s}^{-1}$ either through nucleation or through kinetic particle formation. In this region also ion-induced particle formation can be significant at sulfuric acid concentrations above 10^6 cm^{-3} , but the total particle formation rates are dominated by the neutral pathway.

The full blue area shows the required sulfuric acid concentrations at which ion-induced particle formation takes place in the kinetic regime and at rates above $1 \text{ cm}^{-3} \text{ s}^{-1}$. Kinetic ion-induced particle formation rate is directly proportional to sulfuric acid concentration as well as to ion concentration (equation (16)). The short-dashed black line marks the sulfuric acid concentrations above which ion-induced particle formation is kinetic, including all regions to the left of the line. However, outside of the blue area the ion-induced rate is either less than $1 \text{ cm}^{-3} \text{ s}^{-1}$ (white region) or its contribution to overall particle formation rate is minor compared to neutral particle formation that has a higher proportionality to sulfuric acid concentration (red regions).

The hatched blue area shows the region where ion-induced binary particle formation takes place through nucleation at rates above $1 \text{ cm}^{-3} \text{ s}^{-1}$. In this region particle formation rate is a very steep function of sulfuric acid concentration. Ultimately, the ion-induced particle formation rates are limited by the ion production rate, taken here to be $20 \text{ cm}^{-3} \text{ s}^{-1}$, in the full blue region separated by the long-dashed line. The hatched white area in Figure 8 shows the region where neither neutral nor ion-induced sulfuric acid-water particle formation rate is significant, and it covers the typical conditions in the warm planetary boundary layer.

Overall, Figure 8 shows that neutral and ion-induced particle formation mechanisms can be significant under different atmospheric conditions. Neutral sulfuric acid-water particle formation requires extremely cold temperatures to take place, so the process is limited to regions above the midtroposphere, but the formation rates can be significantly higher than those for ion-induced particle formation due to comparably low number of atmospheric ions and the maximum rate set by the ion production limit. Ion-induced particle formation takes place at warmer temperatures and can be significant at free troposphere and in the boundary layer under cold conditions (roughly below 0°C).

4. Conclusions

We have presented a quantum chemistry-normalized Classical Nucleation Theory of neutral and ion-induced particle formation in the sulfuric acid-water system, where updated quantum chemical reaction coefficients for sulfuric acid hydration are used. The theory is based on the work of *Noppel et al.* [2002], an approach where the liquid droplet model used in CNT is corrected with the use of a reference cluster concentration obtained either from a more refined theory or from experiments. In the neutral case such a cluster concentration can be obtained from quantum chemical calculations, whereas in the ion-induced case the ion concentration itself plays a similar role. The theory describes how the nucleation regime involving a free energy barrier, with a complex and strong dependence of formation rates on sulfuric acid, RH, and temperature, transforms into the barrierless kinetic regime, with little dependence on RH or temperature, and linear (ion-induced case) or quadratic (neutral case) dependence on sulfuric acid. The transition points themselves depend on these same variables, but ion-induced particle formation becomes kinetic at higher temperatures or lower sulfuric acid concentrations than the neutral particle formation. When the binary system is already in the kinetic regime the particle formation rate is likely not greatly enhanced by the presence of another chemical species, as there is no free energy barrier that impedes the binary process.

Observed particle formation in the boundary layer depends on the sulfuric acid concentration to the powers between first and second [*Kulmala et al.*, 2006]. Theoretical binary kinetic-type particle formation requires conditions, however, that are not typically met in the boundary layer. This agrees with observations suggesting that boundary layer particle formation typically requires another component [*Zhang et al.*, 2012]. However, it may well be that multicomponent processes follow similar overall characteristics as the binary processes (such as shown in Figure 8) but at elevated temperatures.

Binary water-sulfuric acid particle formation has been studied for decades both experimentally and theoretically without reaching a firm understanding of the system. Together with companion paper, presenting the most comprehensive set of pure binary particle formation measurements up-to-date, we have shown that a quantitative theoretical understanding of the process can be achieved by making a relatively simple quantum chemistry-based correction to the macroscopic liquid drop model.

Acknowledgments

We would like to thank Ismo Napari for theoretical advice. This research has received funding from Magnus Ehrnrooth Foundation, Kone Foundation, ERC-Starting MOCAPAF grant 57360, ERC-Advanced ATMNUCLE grant 227463, the Academy of Finland (Center of Excellence project 1118615), the Academy of Finland (135054, 133872, 251427, 139656, 139995, 137749, 141217, and 141451), the Vaisala Foundation, the Nessling Foundation, and the U.S. National Science Foundation (grants AGS1136479, CHE1012293, and AGS1447056.) In keeping with AGU's Data Policy, all thermodynamic data used in the calculations are summarized in Table 1, and the computer code used for the calculations is available from the author upon request.

References

- Almeida, J., et al. (2013), Molecular understanding of sulphuric acid-amine particle nucleation in the atmosphere, *Nature*, *502*, 359–363.
- Ayers, G. P., R. W. Gillett, and J. Gras (1980), On the vapor-pressure of sulfuric acid, *Geophys. Res. Lett.*, *7*, 433–436.
- Bazilevskaya, G. A., et al. (2008), Cosmic ray induced ion production in the atmosphere, *Space Sci. Rev.*, *137*, 149–173.
- Brus, D., K. Neitola, A.-P. Hyvärinen, T. Petäjä, J. Vanhanen, M. Sipilä, P. Paasonen, M. Kulmala, and H. Lihavainen (2011), Homogeneous nucleation of sulfuric acid and water at close to atmospherically relevant conditions, *Atmos. Chem. Phys.*, *11*, 5277–5287, doi:10.5194/acp-11-5277-2011.
- Duplissy, J., et al. (2016), Effect of ions on sulfuric acid-water binary particle formation: 2. Experimental data and comparison with QC-normalized classical nucleation theory, *J. Geophys. Res. Atmos.*, *121*, doi:10.1002/2015JD023539.
- Ehrhart, S., and J. Curtius (2013), Influence of aerosol lifetime on the interpretation of nucleation experiments with respect to the first nucleation theorem, *Atmos. Chem. Phys.*, *13*, 11,465–11,471, doi:10.5194/acp-13-11465-2013.
- Eisele, F. L., and D. J. Tanner (1993), Measurement of the gas phase concentration of H₂SO₄ and methane sulfonic acid and estimates of H₂SO₄ production and loss in the atmosphere, *J. Geophys. Res.*, *98*(D5), 9001–9010, doi:10.1029/93JD00031.
- Girshick, S. L., and C.-P. Chiu (1990), Kinetic nucleation theory—A new expression for the rate of homogeneous nucleation from ideal supersaturated vapor, *J. Chem. Phys.*, *93*, 1273–1277.
- Heist, R. H., and H. Reiss (1974), Hydrates in supersaturated binary sulfuric acid vapor, *J. Chem. Phys.*, *61*, 573–581.
- Henschel, H., J. C. A. Navarro, T. Yli-Juuti, O. Kupiainen-Määttä, T. Olenius, I. K. O. Colomer, S. L. Clegg, T. Kurtén, I. Riipinen, and H. Vehkamäki (2014), Hydration of atmospherically relevant molecular clusters: Computational chemistry and classical thermodynamics, *J. Phys. Chem. A*, *118*(14), 2599–2611.
- Hoffmann, W., and F. W. Seeman (1960), Schwefelsäure-Wasser gemischen im temperaturbereich von 15 bis 25 C, *Z. Phys. Chem. Neue Folge*, *24*, 300–306.
- Jaeger-Voirol, A., P. Mirabel, and H. Reiss (1987), Hydrates in supersaturated binary sulfuric acid-water vapor—A reexamination, *J. Chem. Phys.*, *87*, 4849–4852.
- Kashchiev, D. (1982), On the relation between nucleation work, nucleus size, and nucleation rate, *J. Chem. Phys.*, *76*, 5098–5102.
- Kerminen, V.-M., et al. (2012), Cloud condensation nuclei production associated with atmospheric nucleation: A synthesis based on existing literature and new results, *Atmos. Chem. Phys.*, *12*, 12,037–12,059.
- Kirkby, J., et al. (2011), Role of sulphuric acid, ammonia and galactic cosmic rays in atmospheric aerosol nucleation, *Nature*, *476*, 429–433.
- Kuang, C., P. H. McMurry, A. V. McCormick, and F. L. Eisele (2008), Dependence of nucleation rates on sulfuric acid vapor concentration in diverse atmospheric locations, *J. Geophys. Res.*, *113*, 2156–2202, doi:10.1029/2007JD009253.
- Kulmala, M., and A. Laaksonen (1990), Binary nucleation of water sulfuric-acid system: Comparison of classical theories with different H₂SO₄ saturation vapor-pressures, *J. Chem. Phys.*, *93*, 696–701.
- Kulmala, M., M. Lazaridis, A. Laaksonen, and T. Vesala (1991), Extended hydrates interaction model: Hydrate formation and the energetics of binary homogeneous nucleation, *J. Chem. Phys.*, *94*, 7411–7413.
- Kulmala, M., K. E. J. Lehtinen, and A. Laaksonen (2006), Cluster activation theory as an explanation of the linear dependence between formation rate of 3 nm particles and sulphuric acid concentration, *Atmos. Chem. Phys.*, *6*, 787–793.
- Kupiainen-Määttä, O., T. Olenius, H. Korhonen, J. Malila, M. D. Maso, K. Lehtinen, and H. Vehkamäki (2014), Critical cluster size cannot in practice be determined by slope analysis in atmospherically relevant applications, *J. Aerosol Sci.*, *77*, 127–144.
- Kurten, T., M. Noppel, H. Vehkamäki, M. Salonen, and M. Kulmala (2007), Quantum chemical studies of hydrate formation of H₂SO₄ and HSO₄−, *Boreal Environ. Res.*, *12*, 431–453.
- Laakso, L., J. M. Mäkelä, L. Pirjola, and M. Kulmala (2002), Model studies on ion-induced nucleation in the atmosphere, *J. Geophys. Res.*, *107*(D20), 4427, doi:10.1029/2002JD002140.
- Loukonen, V., T. Kurten, I. K. Ortega, H. Vehkamäki, A. A. H. Padua, K. Sellegri, and M. Kulmala (2010), Enhancing effect of dimethylamine in sulfuric acid nucleation in the presence of water—A computational study, *Atmos. Chem. Phys.*, *10*, 4961–4974.
- Lovejoy, E. R., J. Curtius, and K. Froyd (2004), Atmospheric ion-induced nucleation of sulfuric acid and water, *J. Geophys. Res.*, *109*, D08204, doi:10.1029/2003JD004460.
- Määttä, A., H. Vehkamäki, A. Lauri, I. Napari, and M. Kulmala (2007), Two-component heterogeneous nucleation kinetics and an application to Mars, *J. Chem. Phys.*, *127*(13), 134710.
- McMurry, P. H. (1980), Photochemical aerosol formation from SO₂: A theoretical analysis of smog chamber data, *J. Colloid Interface Sci.*, *78*(2), 513–527, doi:10.1016/0021-9797(80)90589-5.
- McMurry, P. H. (1983), New particle formation in the presence of an aerosol: Rates, time scales, and sub-0.01 μm size distributions, *J. Colloid Interface Sci.*, *95*(1), 72–80, doi:10.1016/0021-9797(83)90073-5.
- Merikanto, J., E. Zupadinsky, A. Lauri, and H. Vehkamäki (2007), Origin of the failure of classical nucleation theory: Incorrect description of the smallest clusters, *Phys. Rev. Lett.*, *98*(14), 145702.
- Mikkonen, S., et al. (2011), A statistical proxy for sulphuric acid concentration, *Atmos. Chem. Phys.*, *11*, 11,319–11,334, doi:10.5194/acp-11-11319-2011.
- Morgan, L. J., and C. E. Davies (1916), The properties of mixed liquids: I. Sulfuric acid-water mixtures, *J. Am. Chem. Soc.*, *28*, 555–568.
- Murphy, D. M., and T. Koop (2005), Review of the vapour pressures of ice and supercooled water for atmospheric applications, *Q. J. R. Meteorol. Soc.*, *131*(608), 1539–1565.
- Myhre, C. E. L., C. J. Nielsen, and O. W. Saastad (1998), Density and surface tension of aqueous H₂SO₄ at low temperature, *J. Chem. Eng. Data*, *43*, 617–622.
- National Research Council (1928), *International Critical Tables of Numerical Data Physics, Chemistry and Technology*, vol. 1, Mc Graw-Hill, New York.
- Noppel, M., H. Vehkamäki, and M. Kulmala (2002), An improved model for hydrate formation in sulfuric acid-water nucleation, *J. Chem. Phys.*, *116*, 218–228.

- Olenius, T., O. Kupiainen-Määttä, I. K. Ortega, T. Kurtén, and H. Vehkamäki (2013), Free energy barrier in the growth of sulfuric acid-ammonia and sulfuric acid-dimethylamine clusters, *J. Chem. Phys.*, *139*(8), 084312.
- Pierce, J. R., and P. J. Adams (2009), A computationally efficient aerosol nucleation/condensation method: Pseudo-steady-state sulfuric acid, *Aerosol Sci. Technol.*, *43*, 216–226.
- Pierce, J. R., M. J. Evans, C. E. Scott, S. D. D'Andrea, D. K. Farmer, E. Swietlicki, and D. V. Spracklen (2013), Weak global sensitivity of cloud condensation nuclei and the aerosol indirect effect to Criegee + SO₂ chemistry, *Atmos. Chem. Phys.*, *13*, 3163–3176, doi:10.5194/acp-13-3163-2013.
- Rao, N. P., and P. H. McMurry (1989), Nucleation and growth of aerosol in chemically reacting systems: A theoretical study of the near-collision-controlled regime, *Aerosol Sci. Technol.*, *11*(2), 120–132, doi:10.1080/02786828908959305.
- Reiss, H. (1950), The kinetics of phase transitions in binary systems, *J. Chem. Phys.*, *18*, 840.
- Sabinina, L., and L. Terpugow (1935), Die Oberflächenspannung des Systems Schwefelsäure-Wasser, *Z. Phys. Chem.*, *A173*, 237–241.
- Sipilä, M., et al. (2010), The role of sulfuric acid in atmospheric nucleation, *Science*, *327*, 1243–1246.
- Sorokin, A., F. Arnold, and D. Wiedner (2006), Formation and growth of sulfuric acid-water cluster ions: Experiments, modelling, and implications for ion-induced aerosol formation, *Atmos. Environ.*, *40*, 2030–2045.
- Stauffer, D. (1976), Kinetic theory of two-component (hetero-molecular) nucleation and condensation, *J. Aerosol Sci.*, *7*(4), 319–333.
- Suggitt, R. M., P. M. Aziz, and F. E. W. Wetmore (1949), The surface tension of aqueous sulfuric acid solutions at 25-degrees, *J. Am. Chem. Soc.*, *71*, 676–678.
- Thomson, J. (1906), *Conduction of Electricity Through Gases*, Cambridge Univ. Press, Cambridge.
- Usoskin, I. G., G. A. Kovaltsov, and I. A. Mironova (2010), Cosmic ray induced ionization model CRAC:CRIL: An extension to the upper atmosphere, *J. Geophys. Res.*, *115*, D10302, doi:10.1029/2009JD013142.
- Vehkamäki, H., M. Kulmala, I. Napari, K. E. J. Lehtinen, C. Timmreck, M. Noppel, and A. Laaksonen (2002), An improved parameterization for sulfuric acid-water nucleation rates for tropospheric and stratospheric conditions, *J. Geophys. Res.*, *107*(D22), 4622, doi:10.1029/2002JD002184.
- Vehkamäki, H., M. J. McGrath, T. Kurtén, J. Julin, K. E. J. Lehtinen, and M. Kulmala (2012), Rethinking the application of the first nucleation theorem to particle formation, *J. Chem. Phys.*, *136*(9), 094107.
- Wexler, A. (1976), Vapor pressure formulation for water in range 0 to 100°C: A revision, *J. Res. Natl. Bur. Stand. Sect. A.*, *80*(5–6), 775–785.
- Wilemski, G., and B. E. Wyslouzil (1995), Binary nucleation kinetics: 1. Self-consistent size distribution, *J. Chem. Phys.*, *103*, 1127–1136.
- Yu, F. (2006), From molecular clusters to nanoparticles: Second-generation ion-mediated nucleation model, *Atmos. Chem. Phys.*, *6*, 5193–5211.
- Yu, F. (2010), Ion-mediated nucleation in the atmosphere: Key controlling parameters, implications, and look-up table, *J. Geophys. Res.*, *115*, D03206, doi:10.1029/2009JD012630.
- Yu, F., and R. P. Turco (2011), The size-dependent charge fraction of sub-3-nm particles as a key diagnostic of competitive nucleation mechanisms under atmospheric conditions, *Atmos. Chem. Phys.*, *11*, 9451–9463.
- Yue, G. K., and L. Y. Chan (1979), Theory of the formation of aerosols of volatile binary-solutions through the ion-induced nucleation process, *J. Colloid Interface Sci.*, *68*, 501–507.
- Zeleznik, F. J. (1991), Thermodynamic properties of the aqueous sulfuric-acid system to 350 K, *J. Phys. Chem. Ref. Data*, *20*, 1157–1200.
- Zhang, R. Y., A. Khalizov, L. Wang, M. Hu, and W. Xu (2012), Nucleation and growth of nanoparticles in the atmosphere, *Chem. Rev.*, *112*, 1957–2011.
- Zhang, Y., P. H. McMurry, F. Yu, and M. Z. Jacobson (2010), A comparative study of nucleation parameterizations: 1. Examination and evaluation of the formulations, *J. Geophys. Res.*, *115*, D20212, doi:10.1029/2010JD014150.